Available online at www.sciencedirect.com

SCIENCE DIRECT®

Continental Shelf Research 26 (2006) 1258–1280

CONTINENTAL SHELF RESEARCH

www.elsevier.com/locate/csr

The magnitude and frequency of combined flow bed shear stress as a measure of exposure on the Australian continental shelf

M.A. Hemer*

Marine and Coastal Environment Group, Geoscience Australia, GPO Box 378, Canberra ACT, 2601, Australia

Received 29 November 2005; received in revised form 15 March 2006; accepted 31 March 2006

Abstract

Benthic habitats on the continental shelf are strongly influenced by exposure to the effects of surface ocean waves, and tidal, wind and density driven ocean currents. These processes combine to induce a combined flow bed shear stress upon the seabed which can mobilise sediments or directly influence organisms disturbing the benthic environment. Output from a suite of numerical models predicting these oceanic processes have been utilised to compute the combined flow bed shear stresses over the entire Australian continental shelf for an 8-year period (March 1997–February 2005 inclusive). To quantify the relative influence of extreme or catastrophic combined flow bed shear stress events and more frequent events of smaller magnitude, three methods of classifying the oceanographic levels of exposure are presented: (1) A spectral regionalisation method, (2) A method based on the shape of the probability distribution function, and (3) A method which assesses the balance between the amount of work a stress does on the seabed, and the frequency with which it occurs. Significant relationships occur between the three regionalisation maps indicating seabed exposure to oceanographic processes and physical sediment properties (mean grain size and bulk carbonate content), and water depth, particularly when distinction is made between regions dominated by high-frequency (diurnal or semi-diurnal) events and low-frequency (synoptic or annual) events. It is concluded that both magnitude and frequency of combined-flow bed shear stresses must be considered when characterising the benthic environment. The regionalisation outputs of the Australian continental shelf presented in this study are expected to be of benefit to quantifying exposure of seabed habitats on the continental shelf to oceanographic processes in future habitat classification schemes for marine planning and policy procedures.

Keywords: Exposure; Disturbance; Habitat; Ocean modelling; Continental shelf; Australia

1. Introduction

The merits of habitat classification schemes, and how habitats can be ranked hierarchically, as a means of systematically protecting the marine environment are becoming well recognised (Roff et al., 2003). Detailed studies of biotic communities are a particularly difficult and time-consuming task in the marine environment, and as a result, studies commonly use 'indicator' physical characteristics for the identification and classification of marine habitats, e.g., remote sensing, acoustic geophysical methods are increasingly used as a tool to describe habitat type (Fader et al., 1999; Kostylev et al., 2001). Ecologists have long recognised the relationship between benthic

*Corresponding author at: CSIRO Marine and Atmospheric Research, Castray Esplanade, GPO Box 1538, Hobart, TAS 7001, Australia. Tel.: +61 3 6232 5017; fax: +61 3 6232 5123.

E-mail address: mark.hemer@csiro.au.

0278-4343/$ - see front matter Crown Copyright © 2006 Published by Elsevier Ltd. All rights reserved.
doi:10.1016/j.csr.2006.03.011

marine habitats and communities on the continental shelf, and exposure to oceanographic processes (Connell, 1978; Warwick and Uncles, 1980; Coops et al., 1991; Long et al., 1997; Fonseca and Bell, 1998; Duggins et al., 2001; Edgar, 2001; Goodsell and Connell, 2005; Wernberg and Thomsen, 2005). However, indicator physical characteristics from an oceanographic viewpoint included in habitat classification schemes are typically a qualitative description of mean conditions (e.g., Edgar, 1997, classifies habitats based on wave exposure as sheltered, moderately exposed, sub-maximally exposed, or exposed). At best quantitatively, wave heights, tidal ranges and water depth (Greene et al., 1999; Roff et al., 2003) are included to provide some quantitative estimate of oceanographic processes on benthic conditions. Such an approach does not quantify the shear stress force that acts to disturb the seabed and associated communities. Neither does it consider the well-documented interaction (Grant and Madsen, 1986) between wave-generated oscillatory bottom currents, and unidirectional currents due to tides, winds and other forces. Bio-regionalisation of continental scale shelf regions (where qualitative descriptions may become imprecise) are currently being undertaken in Australia, and elsewhere worldwide, in a new era of ecosystem based marine management and require a quantitative measure of the impact of these physical processes on the seabed and associated benthic habitats.

Exposure to oceanographic processes on the continental shelf includes the action of waves and currents (tidal, wind-driven, geostrophically driven) on the seabed. These processes exert a physical stress on organisms, tearing plants from their place of attachment (Thomsen et al., 2004), mobilising sediment and burying (Aller and Todorov, 1997), damaging organisms by abrasion (Cheroske et al., 2000), or limiting light availability (Carruthers et al., 2002) amongst other mechanisms. The effectiveness of these oceanographic processes to shape benthic habitats involves both the magnitude of the shear stresses, and the frequency with which they occur. For example, storm-dominated shelves are made up of regions impacted upon by regular synoptic scale storms (e.g., the southern Australian margin), regions strongly influenced by seasonal differences (e.g., Torres Strait south-easterly trade and north-westerly monsoon seasons), and regions influenced by the less predictable cyclone systems (e.g., the Gulf of Carpentaria). In a tidally dominated shelf region, any habitat or community will have adapted to the predictable hydrodynamic forces, with the maximum force that a community is likely to have to endure experienced during each spring-neap cycle. A community adapted to large shear stresses which occur every 2 weeks is likely to be very different from a community which experiences the same magnitude shear stress just once a year. Any quantification of exposure to be included in a habitat classification scheme must therefore include some parameterisation of the frequency as well as the magnitude of exposure to these oceanographic wave and current induced stresses.

The population dynamics of benthic marine organisms are controlled by a complex interaction of biological and physical processes. The interaction between the two processes can be non-intuitive, complicating any effort to construct predictive models regarding population and community structure. The biological communities which occupy a particular habitat have adapted to that environment, and the levels of exposure experienced there, through natural selection (Krebs, 1994). Exposure on the seabed to oceanographic processes as quantified within this study is only one of many forces that act to disturb the benthic environment. Hall (1994) reviews the physical and biological processes capable of disturbing benthic communities, including bioturbation, fishing, and dredging, in addition to the oceanographic processes. Disturbance is difficult to quantify when considering a variety of habitats, communities and substrate types (e.g., a stress which disturbs one environment may not disturb another), however relative levels of exposure, and what an environment can withstand is more easily compared. Environmental response to exposure is also not straightforward. The Intermediate Disturbance Hypothesis (Connell, 1978), states that maximum diversity occurs at intermediate levels (magnitude or frequency) of exposure (disturbance) due to biological interactions which take place in response to the disturbances. High bed shear stresses do not necessarily result in disturbance of the seabed. Shear stresses indicate the presence of turbulence in the benthic boundary layer required to keep suspended particulate matter in the water column, which many species depend upon for passive suspension feeding (Hentschel and Larson, 2004). For example, in the deep ocean environment, Aller (1989) observed that periods of low currents speeds (low bed shear stresses) after a benthic storm resulted in rapid deposition of suspended sediments, burying organisms and in-filling burrows (i.e., the relaxation of energetic currents causes the high disturbance event). The regionalisation maps indicating levels of exposure on the seabed of the Australian continental shelf presented in this study are intended to be one data-layer of many which are used to characterise the benthic environment.

Porter-Smith et al. (2004) provided some indication of exposure levels on Australia's continental shelf by estimating the percentage time of sediment mobility with the aim of classifying Australia's shelf as wave or tide dominated. The approach used by Porter-Smith et al. (2004) considers the frequency with which sediments are mobilised, but does not include a measure of intensity. The aim of the present study is to quantify both the frequency and magnitude of combined flow bed shear stresses as a measure of exposure on the Australian continental shelf, and provide a regionalisation that might be used as part of a hierarchical habitat classification scheme. A second aim of the study is to test whether physical sediment properties (grain size and carbonate content) are in hydraulic equilibrium with the prevailing oceanographic conditions. Several previous studies have found that carbonate sediments on the outer portions of the Australian continental shelf are attributed in many areas to their relict origin (e.g., Jones, 1973; Davies, 1979; Jones and Davies, 1983). Porter-Smith et al. (2004) concluded that the mean grain size of bed sediments was not in hydraulic equilibrium with the frequency of wave-induced and tide-induced sediment disturbance events. In this study, this approach is advanced to include both the intensity and frequency of combined-flow bed shear stress events and the influence of oceanic currents in the analysis.

2. Methods

Outputs from a suite of numerical models including wave, tide, and oceanographic circulation models for the Australian region were used as input to a bottom boundary layer model. Hourly estimates of combined wave-current bed shear stress on Australia's continental shelf over an 8 year time period were computed.

2.1. The model and inputs

The wave and tide model used have been previously documented in Porter-Smith et al. (2004). The wave model is a high-resolution (0.1°) application of the WAM wave model (Hasselman and the WAMDI Group, 1988; Komen et al., 1994) for the Australian region (latitudes range from 7°S to 46°S, and longitudes range from 110°E to 156°E), run by the Australian Bureau of Meteorology (Porter-Smith et al., 2004). Wave model hind cast output are 6-hourly predictions of significant wave height (H_s), mean wave period (T_m) and mean wave direction (ϕ_W), gridded at 0.1° spatial resolution, for the period March 1997 to February 2005, inclusive. Wave data were temporally interpolated so that hourly estimates were available to coincide in time with current velocity estimates which incorporate semi-diurnal tidal cycles (see below). In water depths less than 20 m, shallow water effects not parameterised in the model (such as depth-induced breaking) may become important, and the WAM model may become inaccurate (Booij et al., 1999). Using the required input of significant wave height (H_s), period (T), and water depth (h), linear wave theory is implemented to compute hourly maximum bottom wave-orbital velocity at each grid cell on the continental shelf.

The tide model is an application of the linearised, shallow water tide model, described by Egbert et al. (1994), to the Australian region (Porter-Smith et al., 2004). The model region was limited by 0°S to 45°S and 109°E to 160°E, with a spatial resolution of 0.067°. A simple assimilation procedure called blending was used to incorporate TOPEX/POSEIDON altimetry data from a total of 179 crossover solutions, and Australian National Tidal Facility primary port tide gauge data from 16 locations, into the hydrodynamic model. Tide gauge data from 41 remaining ports were used to tune and validate the tide model (Porter-Smith et al., 2004). The model output provides sine and cosines of the east and north components of barotropic velocity for the four main constituents M_2, S_2, K_1 and O_1 on the Australian shelf, and is assumed to represent the tidal currents at 1 m above the seabed. To enable tide conditions to be known at identical locations to wave conditions for input to the bottom boundary layer model (see below), the tide model output was interpolated onto the 0.1° wave grid. Sines and cosines of velocity components were used to calculate hourly tidal current velocities on the Australian shelf for the period of available wave data (March 1997–February 2005).

Output from the OCCAM ocean circulation model (Webb et al., 1998) is used to obtain estimates of seasonal wind and density-driven, near-bed ocean currents on the Australian shelf. Four years of OCCAM output (years 8.0–12.0) are available. However, these years do not correspond in time to the wave data. In this study, the OCCAM data have been used to represent typical climatological (seasonal) currents on the Australian shelf and the 4 years of OCCAM output is simply run through twice during the 8 years of the available wave data. The OCCAM output is available on a 0.25° grid every 15 days. The near-bed velocity was extracted from the output as the velocity in the lowest z-layer above the seabed. In all cases, this velocity was assumed to represent the velocity at 1 m above the seabed. For each time level of OCCAM output, the near-bed velocity was bi-linearly interpolated onto the 0.1° wave grid. The OCCAM output data was then temporally interpolated and linearly vector summed with predicted tidal velocity to obtain an hourly estimate of total current velocity. The main consequence of using the OCCAM model output to represent the oceanic currents is that storm driven currents on the shelf are un-likely to be quantified, thus underestimating combined wave-current bed shear stresses during storm events. However, the influence of wind and density-driven currents at the seabed is generally less than that from tides or waves and the underestimation of wind-driven events is expected to only slightly underestimate combined-flow bed shear stress model outputs.

Due to the depth attenuation of wave orbital velocity, water depth is an important input for the bottom boundary layer model. Water depth (h) was approximated from Geoscience Australia's 250 m spatial resolution bathymetry model. The bathymetry model was re-interpolated to a grid spacing of 0.1° to coincide with the 0.1° wave grid. The region of interest for this study is limited to the Australian continental shelf, as defined by the area where water depth is less than 300 m (Harris et al., 2003; Fig. 1).

To provide an estimate of hydraulic roughness at the seabed on the Australian continental shelf, the observed mean grain size, D, of sediment on the Australian continental shelf was determined (i.e., Roughness length, $z_o = D/30$). Data were provided by the Geoscience Australia marine sediments database (MARS; Geoscience Australia, 2005). All data containing quantitative grain-size data were extracted (~15,000 pts) and mean grain size computed at each location. Mean grain-size data were interpolated onto the 0.1° wave grid using an inverse distance-weighting scheme. In large areas where little to no data were available (e.g., the SW region), a constant grain size equal to the total mean (0.9 mm) was specified. The model output combined-flow bed shear stress was found to be relatively insensitive to changes in mean grain size. Under typical oceanographic conditions, a doubling of grain size increased the combined-flow bed shear stress by approximately 15%.

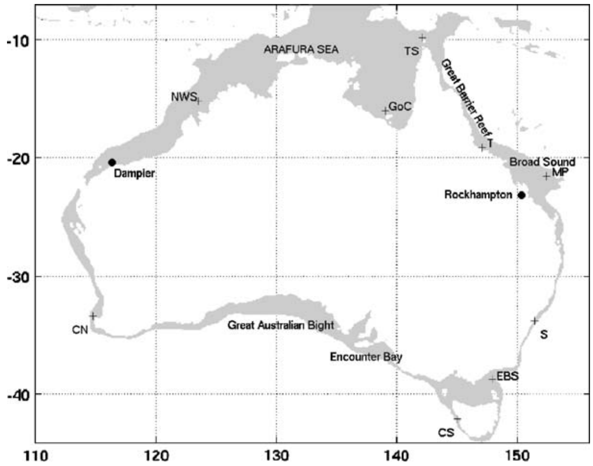

Fig. 1. Map of Australia showing extent of study region (water depth <300 m—shaded), and geographic locations cited in the text. Also shown are the nine sites for which examples are given in Section 3: Cape Sorrell (CS), Cape Naturaliste (CN), Sydney (S), Townsville (T), Marion Plateau (MP), Torres Strait (TS), East Bass Strait (EBS), Gulf of Carpentaria (GoC), and North West Shelf (NWS).

Using these inputs, a one-dimensional bottom boundary layer model was implemented to calculate combined wave-current bed shear stress at each grid cell on the Australian continental shelf. The combined wave-current bottom boundary layer model is based on the SEDTRANS equations detailed by Li and Amos (2001), which is based upon the model developed by Grant and Madsen (1986), but also predicts bedform development, and bedload and suspended load transport for both sand and cohesive sediments. For this study, the combined-flow bed shear stress (τ_{CW}) outputs are considered only, and an 8-year time series of hourly bed shear stresses are calculated at each 0.1° grid cell on the Australian continental shelf (i.e., a total of 24,190 cells).

2.2. *Shelf regionalisation*

The regionalisation of the Australian continental shelf presented by Porter-Smith et al. (2004) is dependent on a grain-size grid containing descriptive data, possibly introducing significant errors. The Porter-Smith et al. (2004) regionalisation is heavily dependent on the threshold exceedance of the sediments, being based on the ratio between waves independently mobilising sediments, and tides independently mobilising sediments. To significantly reduce the dependence on grain size (and consider the interactions which occur between waves and currents), the shelf can be regionalised based on the magnitude and frequency of the combined-flow bed shear stresses, rather than comparing how these stresses exceed the critical threshold for sediment mobility. However if the shelf regionalisation is based only on the magnitude of the mean combined-flow bed shear stress, the influence of extreme storm events (when stresses reach a maximum and the benthic environment is most likely to be disturbed) is limited. Alternatively, if the regionalisation is based only on the magnitude of the maximum stresses recorded on the shelf, very frequent less intense events (e.g., tidal currents) are not accounted for. Consequently, to improve the approach of regionalising the continental shelf based on the exposure of the seabed to oceanographic processes, a method must be devised which quantifies both the magnitude and frequency of the combined-flow bed shear stresses.

In this study, three regionalisation methods are presented which attempt to address these possible sources of error. The first method (the spectral regionalisation) is based on a spectral analysis of the combined-flow bed shear stress, identifying the frequency band in which most energy of shear stress is located, and calculating the total integrated bed shear stress energy. The second method (the PDF regionalisation) identifies the probability distribution of the combined-flow bed shear stress over time, and categorises the shelf based on the shape of the probability distribution curve. The third method (the seabed exposure index regionalisation) calculates the exposure as a function of the product of the bed shear stress probability distribution, and the work the bed shear stresses would do on the shelf to mobilise sediment and/or disturb benthic habitats.

2.2.1. The spectral regionalisation

A spectral analysis was carried out on the combined flow bed shear stress (u and v components) at each grid cell location to determine the energy-frequency distribution. Firstly, the spectrum was partitioned at 33 h period to separate the energy contained within the zone of shorter period (considered high-frequency energy; tidal, or other diurnal or semi-diurnal signature), and the energy contained within the band with longer periods (considered low-frequency synoptic storm or seasonally driven energy). The ratio between energy contained in high and low frequency bands was calculated, and the continental shelf divided into two zones: that where bed shear stress energy is contained mostly in high {low} frequencies. Secondly, the spectrum was integrated over all frequencies to determine the total bed shear stress energy at each location. The 25th and 75th percentiles of bed shear stress energy values on the Australian shelf were determined and the total energy grid was divided into three categories: Low energy locations have total energy less than the 25th percentile; High energy locations have total energy greater than the 75th percentile; and moderate-energy locations have total energy between the 25th and 75th percentiles. The zonings were then combined to create six regions which quantify the magnitude and frequency of bed shear stress events on the Australian continental shelf: Bed shear stress energy contained in low frequency band (0: low, 2: moderate and 4: high-energy zones); bed shear stress contained in high frequency band (1: low, 3: moderate and 5: high-energy zones).

2.2.2. The PDF regionalisation

The data were summarised by four theoretical probability distribution (Gamma; χ^2; Gumbel (Fisher-Tippet type I); and the two-parameter Weibull; Wilks, 1995) to determine which, if any, theoretical distribution provided the best fit to data, enabling two advantages: (1) the shape parameters of the probability distribution function describe the distribution of bed shear stresses succinctly, i.e., reducing the amount of data to be stored to determine probability of a critical shear stress to mobilise bed sediments to occur at a location; and (2) it enables the inverse probability distribution to be determined, i.e., what magnitude stress is achieved X% of the time? The probability distribution can be extrapolated beyond the range of shear stresses for which data is available, and extreme (i.e., N-year return values) events can be predicted.

The two-parameter Weibull distribution was found to provide the best fit of the four tested to the empirical distribution, with goodness-of-fit measured by probability plot correlation coefficient values and the Kolmogorov–Smirnov (K–S) statistic. According to the K–S statistic, the data fit a

Weibull distribution at the 1% significance level over 91% of the Australian continental shelf, and the square of the probability plot correlation coefficient was greater than 0.95% over 92.5% of the shelf area. The two-parameter Weibull distribution is thus considered a good estimate of the combined flow bed shear stress data. Grid cells that do not indicate a good fit to this distribution are predominantly located adjacent to land (<10 m, water depth). A good match in these cells is considered less important given that the reliability of land-adjacent bed shear stresses are questionable due to limitations of the wave model in shallow water and thus likely to contain significant sources of error anyway.

The two-parameter Weibull distribution is described by the cumulative distribution function (CDF) given by

$$\text{Prob}\,(X<x) = F(x) = 1 - \exp(-(x/\beta)^{\alpha}),$$

where α and β are the shape and scale parameters, respectively. α less than or equal to 1 produces reverse J shapes and strong positive skewness in the probability distribution curve. Increasing α acts to increase the slope of the cumulative distribution curve, effectively indicating a smaller data range (Fig. 2). β, the scale parameter, acts to shift the basic shape along the x-axis for a given value of α (i.e., increasing β shifts curve to be more positive, increasing the mean and maximum values; Fig. 2). The distribution of α and β values over the Australian continental shelf can be used to describe the influence of stresses on the shelf. α values greater than one, indicate that bed shear stresses are almost always present at some magnitude (i.e., they are not zero). α values less than one, suggest that bed shear stresses are not always present (i.e., highest probability of being equal to zero). A large β value, in either case indicates that shear stresses have a greater probability of being large. Within this study, the continental shelf is characterised by six conditions describing the frequency and magnitude of stress (Fig. 2):

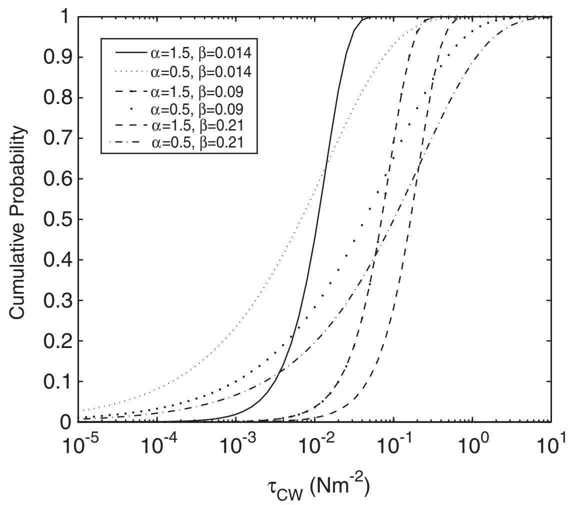

Fig. 2. Representative cumulative distribution curves for six PDF categories. The six categories are represented by: (0) fine dotted line, (1) solid line, (2) coarse dotted line, (3) fine dash–dot line, (4) thick dash–dot line, and (5) dashed line.

0. Large α values ($\alpha>1$), small β values ($\beta \leqslant 25$th percentile): characterise regions where mean bed shear stresses have high probability of being small, and maximum bed shear stresses are also small (i.e., short tail). The probability of zero bed shear stresses occurring is small.
1. Small α values ($\alpha \leqslant 1$), small β values ($\beta \leqslant 25$th percentile): characterises regions where mean bed shear stresses have the greatest probability of being small (or zero). The probability distribution function may have a long positive tail indicating that the site has experienced a relatively large maximum bed shear stress and therefore less frequent storm events may have some influence on the benthic environment in these regions.
2. Large α values ($\alpha>1$), Intermediate β values (25th percentile $<\beta<$75th percentile): characterises regions of the Australian shelf, with mean bed shear stresses in the interquartile range, and maximum bed shear stress is of similar magnitude to the mean. The probability of zero bed shear stresses occurring is small.
3. Small α values ($\alpha \leqslant 1$), intermediate β values (25th percentile $<\beta<$75th percentile): Characterises regions of the Australian shelf, with mean bed shear stresses in the interquartile range. The probability of bed stresses being small (near-zero) is large, however the long tail of the probability distribution indicates the site may experience large maximum bed stresses. Therefore, less frequent, storm events may also have some influence on the benthic environment.
4. Large α values ($\alpha>1$), High β values ($\beta \geqslant 75$th percentile): Characterises regions of the Australian shelf, with high mean bed shear stresses, and maximum bed shear stress is of similar magnitude to the mean. The probability of zero bed shear stresses occurring is small.

5. Small α values ($\alpha \leqslant 1$), High β values ($\beta \geqslant$75th percentile): Characterises regions of the Australian shelf, with high mean bed shear stresses, but the probability of a small bed stress occurring on the seabed is high. The probability distribution function also exhibits a long tail, indicating the site may experience large maximum bed stresses, and therefore less frequent storm events may also have some influence on the benthic environment.

2.2.3. Seabed exposure index

The spectral and PDF regionalisation methods discriminate the continental shelf according to several 'nominal' criteria. In contrast, the seabed exposure index regionalisation is ordinally ranked. This allows a 'sliding scale', so that the relative strength of disturbance may be compared at all sites on the Australian shelf, rather than by comparing zones. The force which acts to disturb the benthic environment is the combined-flow bed shear stress. In the field of sediment transport, it has been argued that the maximum geomorphic/sedimentological work is done when the product of mass rate of sediment transport and the frequency of occurrence is at a maximum (Wolman and Miller, 1960). It is expected that low bed shear stresses which are most frequent, and large bed stresses which occur infrequently, will result in a low value of the mass transport rate times frequency product. McCave (1971) used this approach to show that the mud/sand distribution in the North and Celtic Seas was influenced by the frequency and magnitude of wave events, represented by their near-bed orbital velocity.

Many of the widely used sediment transport formulae (e.g., Bagnold, 1963; Engelund-Hansen, 1967; Yalin, 1963) predict that the sediment transport rate is roughly proportional to the cube of the friction velocity, $u*_{\mathrm{CW}}$, where the friction velocity is defined by

$$u^*_{\mathrm{CW}} = \left(\frac{\tau_{\mathrm{CW}}}{\rho}\right)^{1/2}$$

and ρ is the water density. Thus the sediment transport rate, q, is proportional to $\tau^{1.5}_{\mathrm{CW}}$. Assuming that the work done to disturb the seabed, G, is the same as the work done to transport sediment, then it follows that G is also proportional to $\tau^{1.5}_{\mathrm{CW}}$.

Expressing the percent time for which a given stress is achieved as P, (i.e., the empirical probability distribution function) and following the arguments above, then ($\tau^{1.5}_{\mathrm{CW}}$. P) is proportional to the amount of work done per unit area of seabed by the combined wave-current bed shear stress. This parameter ($\tau^{1.5}_{\mathrm{CW}}$. P) can be viewed as quantifying the level of exposure on the seabed to oceanographic processes, considering both the magnitude and frequency of the bed shear stress. ($\tau^{1.5}_{\mathrm{CW}}$. P) is graphed against τ_{CW}, and the maximum value attained on the curve is termed here as the "seabed exposure index", DE; the stress at which this maximum is achieved is the "effective stress"; and the frequency with which it occurs is the "effective frequency" (Fig. 3).

For this study, the seabed exposure index has been arbitrarily categorised into six equal-area zones to represent different levels of exposure based on cutoffs at the 16th, 33rd, median, 67th, 83rd percentiles of all DE values on the Australian continental shelf: The zones are termed "minimum exposure", "low exposure", "moderately-low exposure", "moderately-high exposure", "high exposure" and "maximum exposure" regions.

2.3. Statistics

The mean water depth, mean mean grain size, and mean carbonate content are calculated for each category within each of the three regionalisation maps. Mean values are determined at those locations only where measurements are available. i.e.,

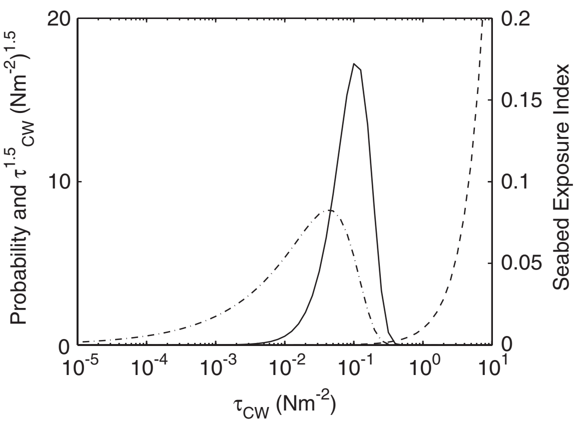

Fig. 3. Relations between frequency of applied stress (the probability distribution, dash–dot line: graphed against LHS y-axis), the work done by the applied stress ($\tau^{1.5}_{\mathrm{CW}}$, dashed line: graphed against the LHS y-axis), and the seabed exposure index (The product of the other two curves, solid line: graphed against RHS y-axis.)

Water depth data are available at all 24,090 locations where the regionalisation are available; mean grain size data are available at 14,828 locations, and carbonate data are available at 4042 locations. For each variable in each of the regionalisations (i.e., nine tests in total), an ANOVA was carried out to determine whether mean values of each variable are significantly different between the zones. A Tukey post-hoc comparison test was carried out to determine which categories have significantly different mean values for each variable. Boxplots are presented to indicate the data range, the interquartile range, and mean and median values for each variable within each category of each regionalisation and serve to show the significant differences between zones in each regionalisation.

2.4. Shelf regionalisation map comparisons

Differences between regionalisation maps created by the three separate methods were quantitatively evaluated using fuzzy set theory (Bandemer and Gottwald, 1995). The three regionalisation methods are not easily compared, as the classification schemes are a mixture of being nominally ranked (e.g., dominated by high- and low-frequency events in the spectral regionalisation) and ordinally ranked (e.g., minimum through to maximum exposure in the seabed exposure index regionalisation). Therefore, comparison of maps should take the fuzziness of the definition of categories into consideration. The method adopted here is outlined by Hagen (2003), and is implemented using the Map Comparison Kit (Visser and de Nijs, 2006). The method considers both fuzziness of location (to account for high spatial variability, or spatial noisiness in the data, not accounted for in cell–cell comparisons), and fuzziness of category.

Differences between three sets of pairs have been determined: (1) spectral to PDF; (2) spectral to seabed exposure index; and (3) PDF to seabed exposure index. The fuzziness of the definition of the categories is incorporated via the category similarity matrix, CSM. In both the spectral and PDF regionalisation schemes, similarity occurs between non-adjacent categories (e.g., the spectral regionalisation: category 0 (low energy dominated by low frequency events) is similarly related to category 2 (mid-energy dominated by low frequency events) and category 1 (low energy dominated by high-frequency events)), and consequently CSM is defined here as:

$$\mathrm{CSM} = \begin{bmatrix} X & A & B & C & 0 & 0 \\ A & X & C & B & 0 & 0 \\ B & C & X & A & B & C \\ C & B & A & X & C & B \\ 0 & 0 & B & C & X & A \\ 0 & 0 & C & B & A & X \end{bmatrix}.$$

Rows of the matrix represent categories of regionalisation scheme 1 and columns of the matrix represent categories of regionalisation scheme 2. X, A, B and C represent the expected probability of a category in scheme 1 to occur in a category of scheme 2 (e.g., the expected probability of category 1 from scheme 1 occurring in category 1 of scheme 2 is X). Several values of X, A, B and C were tested to assess the sensitivity of the analysis, but to indicate the relative differences between schemes, only the case of $X = 1$, $A = 0.7$, $B = 0.4$, and $C = 0.1$ is presented here. The fuzzy membership function used is that of exponential decay with a halving distance of two cells and a neighbourhood with a four cell radius (Hagen, 2003).

The fuzzy comparison produces a map, which specifies the similarity (on a scale of 0–1) for each cell, and an overall value for similarity, K-fuzzy, which is the fuzzy equivalent of the Kappa statistic (which is commonly used in spatial cell–cell comparisons of maps using the same categories (Monserud and Leemans, 1992)).

3. Results

3.1. Site location examples

To demonstrate how each regionalisation scheme categorises a site on the basis of the oceanographic conditions, nine locations were arbitrarily selected to represent a range of different oceanographic conditions (wave/tide/ocean dominated regimes) known to occur on the Australian continental shelf (Porter-Smith et al., 2004; Fig. 1).

Cape Sorrell and Cape Naturaliste (Fig. 1), both on the southern margin of the continent, can be described to be similar under present classification schemes. The Cape Sorrell location lies 10 km west of land, and the Cape Naturaliste location lies 25 km west of land. Surface wave conditions (displayed in Table 1) and tidal ranges (~1 m, Easton, 1970) are similar at both locations. Table 1 however, exhibits two key differences between the two sites which alter their classification: (1) water depth is much greater at the Cape Sorrell site (107 m) than at the Cape Naturaliste site (48 m), indicating a steeper shelf on the western margin of Tasmania and (2) absolute current speeds are much greater at the Cape Naturaliste site (due to the presence of the Leeuwin current moving onto the continental shelf near Cape Naturaliste). The influence these differences have on the bed shear stress energy is demonstrated by Cape Naturaliste being a high-energy site in all three regionalisation methods, and Cape Sorrell being a low energy site in all three regionalisation methods. Both locations have bed shear stress energy mostly contained within synoptic and seasonal frequency bands (Fig. 4), with very little contained in the higher frequency band of periods <33 h. The difference in magnitude (mean and maximum) of bed shear stress energy for the sites is indicated by the larger β values at the Cape Naturaliste site (β: 0.722, as opposed to β: 0.016 at Cape Sorrell; Fig. 5). α values are similar at the two sites (α: 0.634 and α: 0.523 at Cape Naturaliste and Cape Sorrell, respectively), indicating the variance at each site is similar. The three regionalisation schemes all identify differences in seabed exposure between the two southern margin sites (Cape Sorrell and Cape Naturaliste), displaying their usefulness over present qualitative classification schemes.

East Bass Strait and the North-West Shelf contain more energy in the higher frequency band where periods are <33 h. Oceanographic conditions and water depth at these two sites are similar (Table 1), and consequently the combined flow bed shear stress CDF (Figs. 5G and I) and resultant categorisation as moderately high-energy exposure sites dominated by high-frequency events (Table 1) are also similar. Relatively low energy is contained in the lower frequency band at these two sites (Fig. 4G and I).

Four locations are categorised as high-energy exposure sites. Cape Naturaliste has both high mean and maximum combined flow bed shear stresses (Table 1) which are likely to result from the steady flow of the Leeuwin Current, and storms which impact the south-west Australian margin. Townsville and Marion Plateau exhibit similar characteristics with relatively high means and high maximum bed shear stresses. Marion Plateau has the largest maximum combined flow bed shear stress. Hence the shape parameter α, in the theoretical CDF, is reduced indicating greater variance in the data with respect to Townsville (Fig. 5). The Torres Strait site also has relatively high mean and maximum bed shear stresses, but the lower maximum bed shear stress would suggest consistently higher bed shear stresses than at other sites. The lower α value (Fig. 5) at the Torres Strait site indicates that the variance is relatively large in comparison to Townsville and Marion Plateau, and thus indicates small stresses are experienced at this site relatively regularly (e.g., slack tide). The peak in energy with annual period at Torres Strait indicates a strong seasonal signal in the strait consistent with the combined-flow bed shear stress time-series (not shown) which exhibits low bed shear stresses during the Monsoon (December–March) season, and high bed shear stresses during the Trades season (April–November). These results indicate strong seasonal differences in the forces experienced at the seabed in Torres Strait and are supported by observations of seasonal changes in sandwave asymmetry (Harris, 1991). Despite most energy being contained in the lower frequency (seasonal) band in Torres Strait, significant energy peaks are observed at the diurnal and semi-diurnal frequencies owing to the strong tidal currents in the Strait (Fig. 4F). This distribution of energy is expected after previous studies in Torres Strait (Wolanski et al., 1988; Hemer et al., 2004).

No clear relationship is observed between mean or maximum values of each oceanographic process (which are included in present day habitat classification schemes) and the combined-flow bed shear stress which quantifies the effects of all processes on the seabed (Table 1). Given that each categorisation derives directly from the combined-flow bed shear stress, some correlation is expected, and observed, between the categories and shear stress values. It is worthwhile comparing the Gulf of Carpentaria and East Bass Strait sites. Mean combined flow bed shear stresses at the two sites are approximately equal (5% greater at the Bass Strait site than the Gulf of Carpentaria site, Table 1). However, the maximum bed shear stress is three times greater at the Gulf of Carpentaria site than at Bass Strait (Table 1). Regardless of the large maximum event in the Gulf of Carpentaria, the site is categorised as mid-low exposure, dominated by energy in the low-frequency band. Bass Strait is categorised as high exposure, dominated by energy in the high-frequency band. The influence of frequency of bed

Table 1
Mean (denoted by vertical bars) and maximum (denoted by subscript M) oceanographic conditions (mean wave period, T_m, significant wave height, H_s, absolute current speed, u_Z, and water depth, Z) at the nine sites indicated in Fig. 1

	Z (m)	$\|T_m\|$ (s)	$T_{m,M}$ (s)	$\|H_s\|$ (m)	$H_{s,M}$ (m)	$\|u_Z\|$ (m/s)	$u_{Z,M}$ (m/s)	$\|\tau_{CW}\|$ (Nm^{-2})	$\tau_{CW,M}$ (Nm^{-2})	SPEC	PDF	ED	Description of site
Cape Sorrell	107	8.3	14.9	2.4	10.0	0.018	0.059	0.0078	4.06	0	1	1	Low energy exposure site dominated by low frequency (storm/seasonal) events
Cape Naturaliste	48	7.5	15.7	2.2	11.5	0.11	0.27	1.20	85.9	4	5	5	High energy exposure site dominated by low frequency (storm/seasonal) events
Sydney	83	7.1	13.3	1.5	10.3	0.032	0.09	0.012	8.06	2	1	0	Low energy exposure site dominated by low frequency (storm/seasonal) events
Townsville	13	5.8	10.9	1.0	4.4	0.045	0.14	0.42	40.6	4	4	5	High energy exposure site dominated by low frequency (storm/seasonal) events
Marion Plateau	16	6.7	13.1	0.5	6.0	0.072	0.12	0.42	90.4	4	4	5	High energy exposure site dominated by low frequency (storm/seasonal) events
Torres Strait	10	3.6	8.0	0.6	2.6	0.24	0.42	0.46	18.7	4	5	5	High energy exposure site dominated by low frequency (storm/seasonal) events
East Bass Strait	72	6.5	12.2	1.6	7.1	0.14	0.34	0.060	4.22	3	3	4	Mid-High energy exposure site dominated by high frequency (diurnal/semi-diurnal) events
Gulf of Carpentaria	27	3.9	9.5	0.7	4.6	0.066	0.21	0.057	12.2	2	3	2	Mid energy exposure site dominated by low frequency (storm/seasonal) events
North West Shelf	59	5.5	13.2	0.8	7.6	0.15	0.40	0.081	4.10	3	3	4	Mid-High energy exposure site dominated by high frequency (diurnal/semi-diurnal) events

Mean and maximum combined-flow bed shear stress (τ_{CW}) values are shown also, along with how each site is categorised by each of the three regionalisations (the spectral regionalisation SPEC, the PDF regionalisation PDF, and the seabed exposure index regionalisation ED). A final 'summary description' of that site from the categorisation is given.

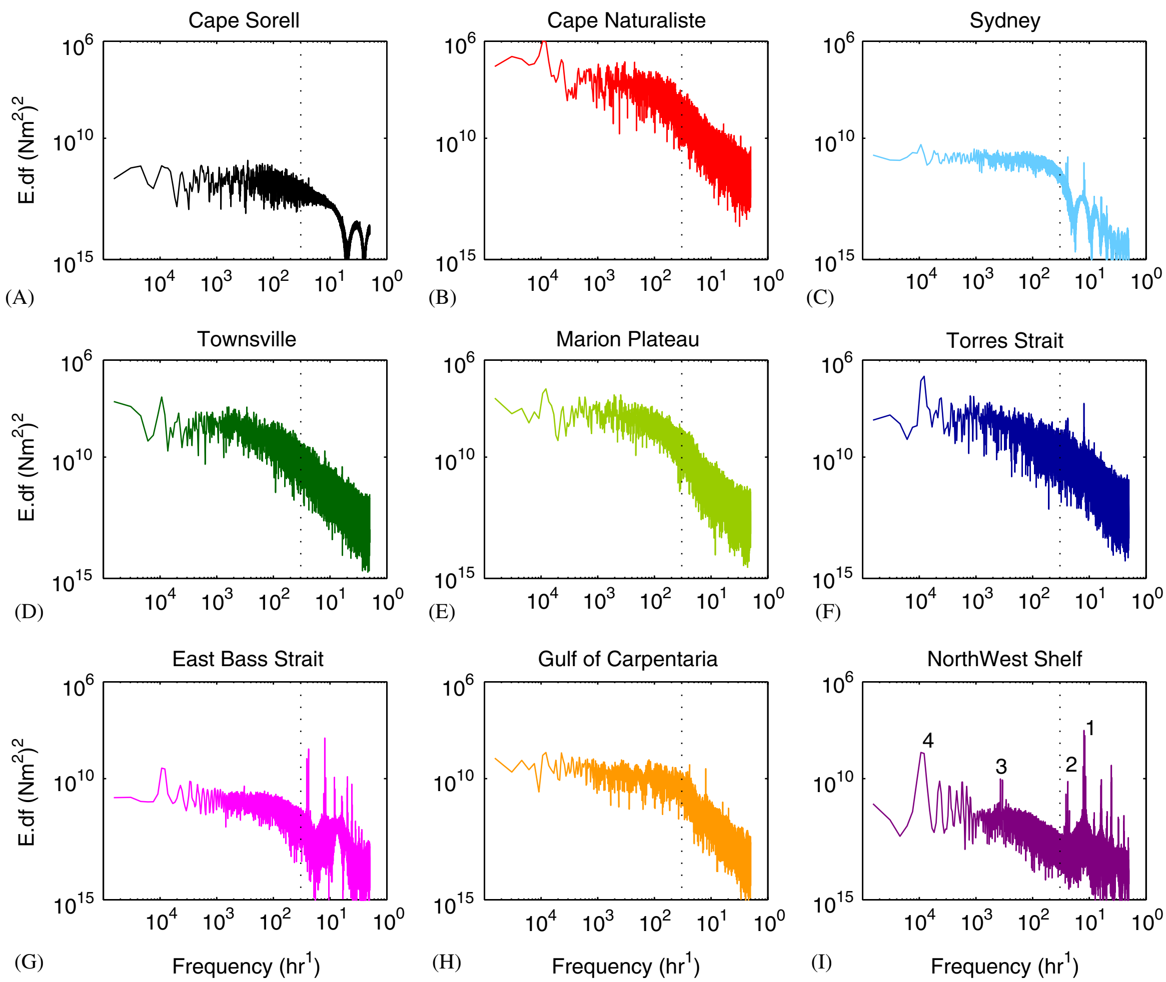

Fig. 4. Combined flow bed shear stress energy spectra at nine example sites: (A) Cape Sorrell (CS), (B) Cape Naturaliste (CN), (C) Sydney (S), (D) Townsille (T), (E) Marion Plateau (MP), (F) Torres Strait (TS), (G) East Bass Strait (EBS), (H) Gulf of Carpentaria (GoC), and (I) North-West Shelf (NWS). The dotted line indicates the 33 h cut-off frequency separating high- and low-frequency energy. Subplot (I) labels four frequencies at which peaks are observed. The peaks may be identified at several of the other locations also. These are: (1) semi-diurnal peak, (2) diurnal peak, (3) spring-neap (14 day) peak, and (4) annual (365 days) peak.

shear stress events and the effectiveness of working the seabed, which cannot be derived from mean and maximum values, is thus clearly illustrated. Bass Strait is impacted upon regularly by moderately large tidal currents, and Gulf of Carpentaria is impacted upon on rare occasions by cyclones. The categorisation procedures outlined in this study allow a quantitative comparison of integrated exposure of benthic environments to oceanographic processes.

3.2. Spectral regionalisation

Total integrated energy distribution on the Australian continental shelf has a maximum value of 0.545 $(\mathrm{Nm}^{-2})^2$. The 25th and 75th percentiles define the inter-quartile range, and separate low, mid and high-energy zones of the spectral regionalisation. Values are 1.44×10^{-8} $(\mathrm{Nm}^{-2})^2$ and 1.51×10^{-6} $(\mathrm{Nm}^{-2})^2$, respectively, on the Australian continental shelf.

The spectral regionalisation (Fig. 6A) is in qualitative agreement with results presented by Porter-Smith et al. (2004) with regions containing energy predominantly in the higher frequency band (Period <33 h) corresponding to Porter-Smith et al. 'Tide dominated' or 'Tide Only' regions. Bed shear stress energy is contained within higher frequencies (light blue, yellow and brown, Fig. 6A) on the mid to outer shelf of Northern Australia extending from

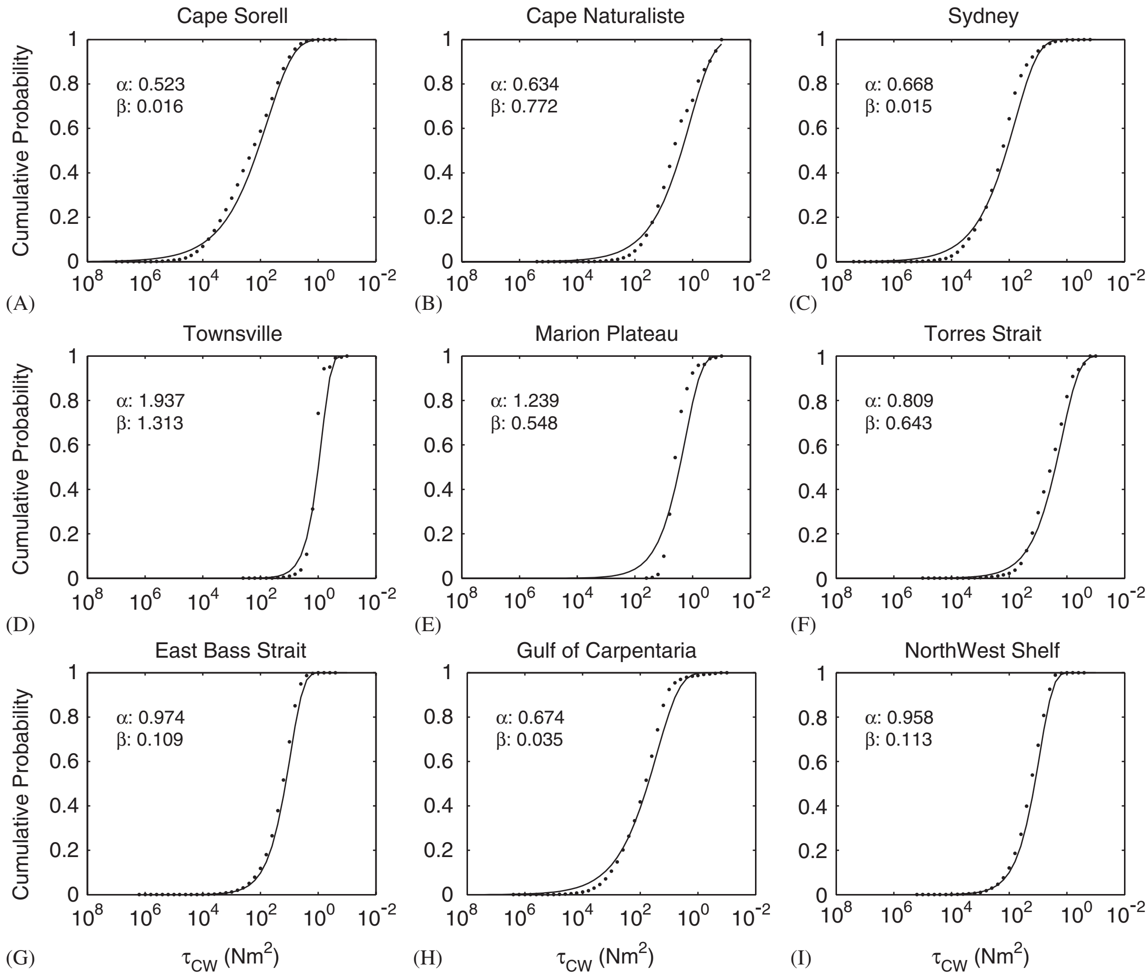

Fig. 5. Cumulative probability distribution function (CDF) at nine example sites: (A) Cape Sorrell (CS), (B) Cape Naturaliste (CN), (C) Sydney (S), (D) Townsille (T), (E) Marion Plateau (MP), (F) Torres Strait (TS), (G) East Bass Strait (EBS), (H) Gulf of Carpentaria (GoC), (I) North-West Shelf (NWS). Dots indicate the empirical CDF with range of values indicated by range of dots, and the solid line indicates the theoretical two-parameter Weibull CDF, with α and β values displayed. The shape parameter α has the effect of changing the slope of the CDF; increasing α values increases slope, or results in a smaller variance reducing tail length. The scale parameter β has the effect of shifting the curve along the x-axis; increasing β shifts CDF towards higher bed shear stresses.

the Gulf of Carpentaria westwards to Dampier, Western Australia. Other areas described by higher frequency bed shear stress energy include areas of Bass Strait and Broad Sound. 'Wave-dominated' or 'wave-only' regions described by Porter-Smith et al. correspond to areas with energy contained within the lower frequency band (Period >33 h, i.e., synoptic storms, seasonal variability, or steady density-driven flows). Bed shear stress energy is dominated by lower frequency events on the inner shelf for almost the entire continent. Aside from some small exceptions (within Bass Strait and the South Australian Gulfs), the entire western, southern, and south-eastern continental shelf margins, extending from Dampier, Western Australia to Rockhampton, Queensland have combined-flow bed shear stress energy contained in lower frequencies (dark blue, green and red, Fig. 6A). Torres Strait and the Northern Great Barrier Reef are also characterised by low-frequency bed shear stress energy, however spatial 'noisiness' between high and low frequency energy regions confirms these regions as 'mixed' wave and tide influenced sites, as categorised by Porter-Smith et al. (2004).

High-energy zones in the spectral regionalisation are predominantly lower frequency regions on the

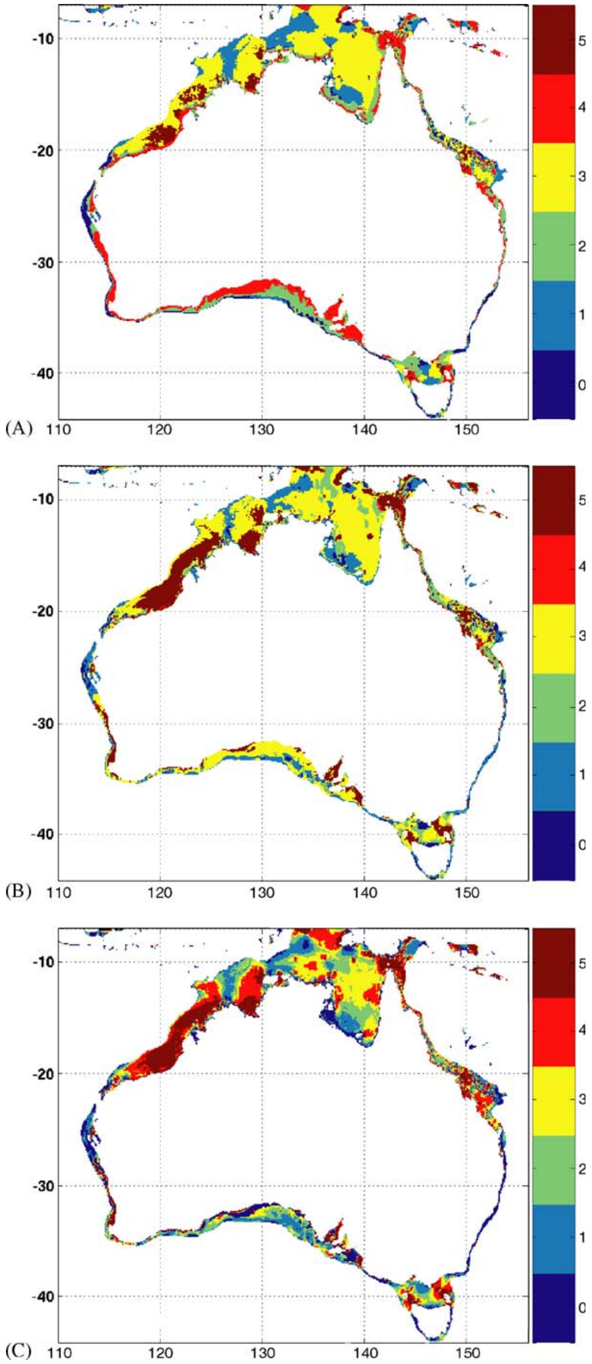

Fig. 6. Regionalisation of the Australian continental shelf, representing the magnitude and frequency of bed shear stress as a measure of exposure: (A) the spectral regionalisation, (B) the PDF regionalisation, and (C) the seabed exposure index regionalisation. Categories for each regionalisation are outlined in Tables 2–4, respectively. Note the different colorscales on each plot, altered to allow some comparison of total energy between methods.

inner shelf (red in Fig. 6A) and higher frequency regions on the mid shelf on the NW Shelf, Broad Sound, and Bass Strait (brown in Fig. 6A). Cross shelf gradients in energy are observed on the entire Australian continental shelf. Low energy zones are predominantly on the outer shelf (Categories 0 and 1, Mean Water Depth ~115 and 114 m, respectively.) The low energy zones (categories 0 and 1) correspond with regions of zero mobility (Porter-Smith et al., 2004), as regions of the Australian continental shelf where bed shear stresses are insufficient to mobilise sediment on the seabed. This result indicates that the zero mobilisation regions are a result of the hydrodynamic conditions being insufficient to create large bed shear stresses rather than an effect of increased grain size in these areas as inferred by Porter-Smith et al. (2004).

Mean water depth, grain size and bulk carbonate content within each category of the spectral regionalisation are detailed in Table 2. The data distribution (interquartile range and general range) for each variable within each category is shown in boxplots (Fig. 7A, D, G). General trends observed are that bed shear stress energy increases with decreasing mean water depth and that in low-frequency energy (e.g. storm) dominated regions, the mean water depth is significantly greater than in high-frequency energy (e.g. tidal) dominated regions (Fig. 7G).

In high-frequency energy dominated regions, no trend is observed in mean grain size with changing bed shear stress energy. However, in low-frequency energy dominated regions, mean grain size displays a significant increasing trend with increasing energy (Fig. 7A).

Significant differences are observed in carbonate content between high- and low-frequency energy dominated regions. Although no significant trends are observed with changing energy, mean carbonate content is observed to increase with increasing energy in high-frequency energy dominated regions (Fig. 7D). No such trend is observed in low-frequency energy dominated regions.

3.3. PDF regionalisation

The scale parameter β has a range of values from 1.21×10^{-10} to 140.9. The 25th and 75th percentiles defining the inter-quartile range of β are used to separate categories of the PDF regionalisation and are 0.030 and 0.167, respectively.

Table 2
Percentage of the Australian continental shelf contained within each category of the spectral regionalisation

	% of total shelf area[a]	Water depth (m)	Mean grain size (mm)	Carbonate content (%)	Median energy $(Nm^{-2})^2$
Cat. 0: low E, low frequency	9.57	114.56 (2361)	**0.557** (4458)	57.25 (651)	2.9313×10^{-9}
Cat. 1: low E, high frequency	15.53	114.10 (3661)	0.329 (1331)	64.82 (708)	4.9366×10^{-9}
Cat. 2: mid E, low frequency	19.26	**53.16** (4787)	**1.103** (3384)	53.11 (839)	4.1457×10^{-7}
Cat. 3: mid E, high frequency	31.31	74.93 (7259)	0.294 (1521)	70.25 (910)	2.0085×10^{-7}
Cat. 4: hi E, low frequency	18.13	**31.35** (4567)	**1.638** (3750)	56.16 (706)	3.0584×10^{-5}
Cat. 5: hi E, high frequency	6.19	57.83 (1455)	0.389 (385)	73.57 (229)	4.8803×10^{-4}
F		1630.76	236.53	54.65	
P		<0.001	<0.001	<0.001	

The mean water depth, the mean mean grain size, and mean bulk carbonate content value within each category. Number in brackets indicates the number of samples contained in category. Bold text indicates that the population of samples contained within the category has a mean value significantly different to the mean of the other categories according to the ANOVA post-hoc comparison Tukey test. F is the ratio of variances with higher values indicating greater variance between categories than within categories, and P indicates the probability level. Mean integrated spectral energy for each category is shown in the last column.

[a]Total shelf area: $2.7581\times10^6\,km^2$.

The PDF regionalisation (Fig. 6B) indicates that the shape parameter α is less than 1 (the probability distribution function exhibits a J-shape) over 80% of the continental shelf (Table 3; light blue, yellow and brown, Fig. 6B). Higher bed shear stress energy regions are associated with greater scale parameter β values in categories 4 and 5 which occur on the NW Shelf, Torres Strait, Broad Sound, Bass Strait, and the inner shelf of the south and western shelf margins (brown and red, Fig. 6B). Low β values (categories 0 and 1, dark and light blue, Fig. 6B) correspond with the low energy zones defined by the spectral regionalisation, occurring on the outer shelf, in the south-west corner of the Gulf of Carpentaria, the central basin of Bass Strait, the Arafura Sea, and a cross shelf 'ribbon' at approximately 126°E in Northern Western Australia. It is apparent there is little difference between high frequency (e.g., tidal) and lower frequency bed shear stresses (e.g., storms) in the PDF regionalisation. Regions with α values greater than 1 (categories 0, 2 and 4), which are predominantly located on the outer shelf or along the Great Barrier Reef, indicate stresses have less variance than regions with low α values.

Mean water depths significantly decrease with increasing β values (i.e., with increasing mean and maximum τ_{cw}, Table 3). The deepest mean water depth identifies with category 0 which has α value greater than 1, but small β values. This category identifies with the smallest mean shear stress, and the shortest PDF tail (smallest maximum bed shear stress values).

Category 4 ($\alpha>1$, large β), is associated with the significantly largest mean grain size (Table 3). The smallest mean grain sizes are associated with categories 0 and 2, which have α greater than 1, and β less than the 25th percentile, or between the 25th and 75th percentiles, respectively, which are likely to have the shortest PDF tails of the six categories (i.e., smallest maximum bed shear stress values). For $\alpha<1$, a significant trend of increasing mean grain size with increasing β is observed.

Although not significant, a positive correlation is observed between the β value of a category and mean carbonate content (Table 3). Increasing β indicates an increase in both the mean and maximum bed shear stress at the site. Category 1 (small α, small β) contains the lowest mean carbonate content, and has the lowest mean bed shear stress of the four categories.

3.4. Seabed exposure index

The seabed exposure index regionalisation (Fig. 6C) shows that regions with greatest exposure are those areas with high frequency (e.g. tidal) bed shear stresses (NW Shelf, Bass Strait and Broad Sound), and those areas which are more strongly influenced by storms or seasonal changes which occur less often, but are likely to have larger bed shear stresses (Torres Strait, Inner shelf on the south and south-west margins).

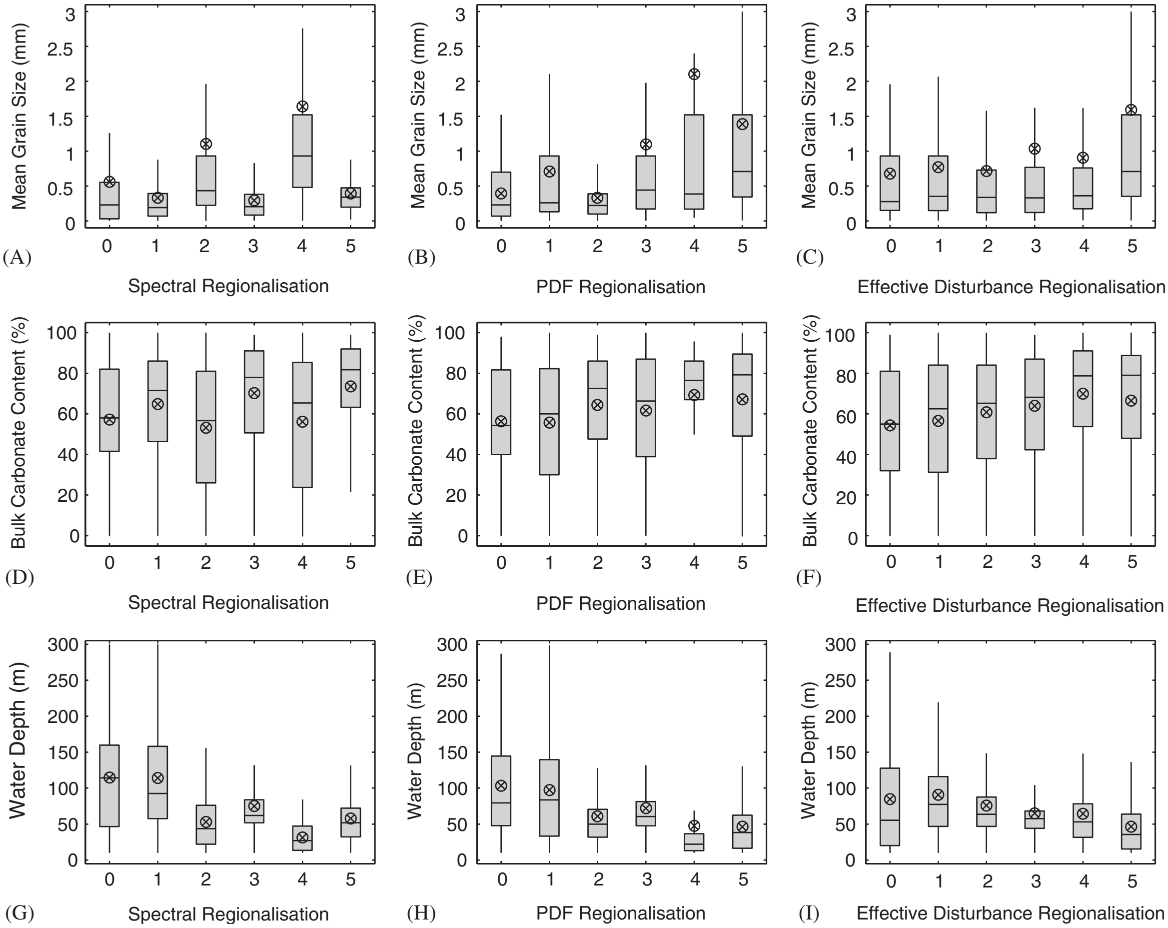

Fig. 7. Boxplots indicating range of water depth, mean grain size and carbonate content data contained within each category for each regionalisation. (A–C) show mean grain size data range for the spectral, PDF, and seabed exposure index regionalisation categories, respectively. (D–F) show bulk carbonate content data range for the three regionalisation categories, and (G–I) show water depth data range for the three regionalisation categories. In each subplot, the box indicates the interquartile range of the variable within each category. The horizontal line indicates the median value in the category, the cross-circle indicates the mean value in the category. The whiskers indicate the general data range of the variable within the category.

Table 3
As for Table 2 for the PDF regionalisation

	% of total shelf area[a]	Water depth (m)	Mean grain size (mm)	Carbonate content (%)	$\langle\alpha\rangle$	$\langle\beta\rangle$
Cat. 0: $\alpha\geqslant 1$, $\beta\leqslant$25th	5.26	**103.60** (1292)	0.392 (1616)	56.31 (439)	1.1787	0.0163
Cat. 1: $\alpha<1$, $\beta\leqslant$25th[b]	19.61	**97.57** (4730)	**0.71** (5288)	55.69 (967)	0.6997	0.0135
Cat. 2: $\alpha\geqslant 1$, 25th $<\beta<$75th	10.60	**61.09** (2557)	0.327 (1169)	64.40 (412)	1.1505	0.0749
Cat. 3: $\alpha<1$, 25th$<\beta<$75th	39.58	**71.99** (9489)	**1.096** (3100)	61.52 (1142)	0.7790	0.0752
Cat. 4: $\alpha\geqslant 1$, $\beta\geqslant$75th	1.54	47.64 (363)	**2.107** (213)	69.33 (50)	1.2409	1.4670
Cat. 5: $\alpha<1$, $\beta\geqslant$75th	23.41	46.28 (5659)	**1.387** (3443)	67.09 (1033)	0.6738	1.0453
F		578.54	134.94	21.67		
P		<0.001	<0.001	<0.001		

Mean shape (α) and scale (β) parameter values for each category are shown in the last two columns.

[a]Total shelf area: $2.7581\times 10^{6}\,km^{2}$.

[b]*Note*: 25th and 75th indicate the respective percentile values, calculated from all β values recorded on the Australian continental shelf.

Category 5, describing highest exposure, has significantly shallowest water depths and significantly largest mean grain sizes (Table 4).

Aside from category 0 which describes the smallest seabed exposure index, water depth shows a general decreasing trend with increasing exposure (Table 4). An increasing trend in mean grain size with increased exposure is observed, however, categories 2 and 4 do not fit this trend.

An increasing trend in carbonate content is observed with increasing exposure for all categories but 5 (which describes the highest effective disturbance sites; Table 4). The results of the post-hoc tukey comparison test indicate that every second category is significantly different, but the differences in mean values between adjacent categories are not significant.

3.5. Statistics

For all of water depth, mean grain size, and bulk carbonate content, the largest F values are associated with the spectral regionalisation (cf. Tables 2–4). The larger F value indicates that the variance between means with respect to the variance within each category is greater for the spectral regionalisation than for the other two methods.

3.6. Shelf regionalisation map comparisons

To identify regions of difference between regionalisation schemes, three pairs of maps were quantitatively compared: (1) spectral to PDF, (2) spectral to seabed exposure, and (3) PDF to seabed exposure. Contingency tables (Tables 5–7 for each map pair, respectively, after Monserud and Leemans, 1992) are presented to indicate how the distribution of categories in map 1 differs to map 2 as a cell-cell comparison. Figs. 8a–c display similarity maps determined using the fuzzy κ test for each map pair, respectively, and identify regions of key difference between map categorisation schemes.

Comparison of the Spectral and PDF regionalisation schemes (Fig. 8a) indicate that similarity values are in excess of 0.65% over 72% of the shelf area. The schemes are most dissimilar in the southern Gulf of Carpentaria and the western Great Australian Bight and in Encounter Bay, South Australia, where similarity values are approximately 0.1. These are all regions which the Spectral scheme defines as mid-high energy, dominated by low-frequency synoptic or seasonal scale events (categories 2 and 4). The PDF scheme defines these

Table 5
Contingency table for spectral to PDF map comparison

PDF/Spectral	0	1	2	3	4	5
0	**2.32**	1.84	1.17	0.0208	0.0083	0
1	5.49	**7.60**	5.89	0.116	0.531	0
2	0.963	1.26	**4.49**	3.308	0.598	0
3	0.980	3.68	6.87	**21.0**	6.90	0
4	0.00830	0	0.511	0.014	**0.772**	0.0747
5	0.0332	0.818	0.938	5.59	**10.1**	5.97

Top row indicates category in spectral regionalisation. Left column indicates category in PDF regionalisation. Numbers in table are percentage of shelf area (%) that lies within categories for each scheme. Bold numbers indicate greatest percentage for given PDF category.

Table 4
As for Table 2 for the seabed exposure index regionalisation

	% of total shelf area	Water depth (m)	Mean grain size (mm)	Carbonate content (%)	⟨DE⟩	$\langle \tau_{cw} \rangle$ (Nm^{-2})
Cat. 0: min. exposure	16.68	**84.74** (4095)	0.677 (5581)	54.34 (938)	1.92×10^{-4}	9.71×10^{-9}
Cat. 1: low exposure	15.85	**90.68** (3855)	0.768 (2630)	56.63 (724)	0.0016	6.81×10^{-9}
Cat. 2: mid-low exposure	16.93	**75.95** (4095)	0.711 (1285)	60.77 (527)	0.0043	1.11×10^{-8}
Cat. 3: mid-high expos.	17.25	65.10 (4095)	1.036 (1270)	63.90 (456)	0.0089	1.68×10^{-8}
Cat. 4: high exposure	16.29	64.58 (3855)	0.904 (1608)	69.85 (609)	0.0244	3.41×10^{-8}
Cat. 5: max. exposure	17.00	**46.59** (4095)	**1.594** (2455)	66.51 (789)	1.2651	2.94×10^{-7}
F		326.57	93.68	34.51		
P		<0.001	<0.001	<0.001		

Mean seabed exposure index (DE) and combined flow bed shear stress (τ_{CW}) values for each category are shown in the last two columns.* Total shelf area: 2.7581×10^{6} km^2.

Table 6
Contingency table for spectral to seabed exposure (SE) map comparison

SE/Spectral	0	1	2	3	4	5
0	**5.28**	4.24	3.03	0.0332	4.41	0
1	2.85	**6.99**	5.32	0.170	0.681	0
2	1.33	3.93	4.78	**5.32**	1.64	0
3	0.282	0.0415	3.23	**11.32**	2.11	0.0083
4	0.0498	0	2.73	**10.17**	2.94	0.116
5	0.0083	0	0.776	3.12	**7.18**	5.92

Top row indicates category in spectral regionalisation. Left column indicates category in seabed exposure regionalisation. Numbers in table are percentage of shelf area (%) that lies within categories for each scheme. Bold numbers indicate greatest percentage for given seabed exposure category.

Table 7
Contingency table for PDF to seabed exposure map comparison

PDF/SE	0	1	2	3	4	5
0	2.51	**2.85**	0	0	0	0
1	**9.39**	9.22	0.606	0.0706	0.0789	0.274
2	0	1.52	**3.61**	3.59	1.90	0
3	3.29	2.05	12.4	**12.9**	8.57	0.120
4	0	0	0	0.0042	**0.917**	0.585
5	1.810	0.374	0.336	0.415	4.54	**16.0**

Top row indicates category in seabed exposure (SE) regionalisation. Left column indicates category in PDF regionalisation. Numbers in table are percentage of shelf area (%) that lies within categories for each scheme. Bold numbers indicate greatest percentage for given PDF category.

regions to have small α values, but a range of β values (categories 1, 3 and 5). The corresponding contingency table (Table 5) indicates that the discrepancy exists since the PDF scheme is heavily biased towards small α values with PDF categories 1, 3 and 5 accounting for 83% of the shelf area. The small α values suggest large but rare (low frequency) storms are influential (i.e., the probability distribution function has a long tail). The spectral regionalisation, however, suggests that only 47% of the shelf area is dominated by low-frequency events. As a result, large areas (45% of the shelf area) are defined as both dominated by high-frequency events (spectral categories 1, 3 and 5) and displaying a long probability distribution function tail (small α, PDF categories 1, 3 and 5). The length of the probability distribution function does not indicate that low-frequency events dominate bed shear stresses on the continental shelf, but simply that these less frequent events are likely to have some influence on the benthic environment.

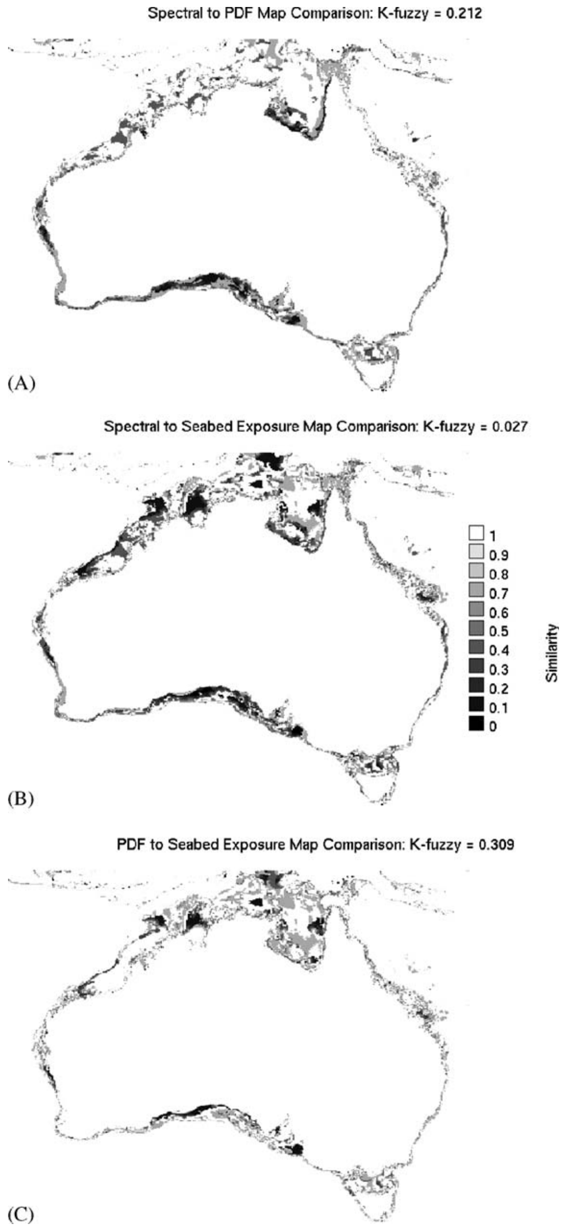

Fig. 8. Results of the fuzzy comparison for regionalisation map pairs: (A) spectral to PDF, (B) spectral to seabed exposure index, and (C) PDF to seabed exposure index. Low similarity values (dark shades) indicate regions of least agreement between regionalisation schemes. *K*-fuzzy statistics are also shown to provide a relative indication of map agreement with an arbitrarily defined category similarity matrix (CSM).

Comparison of the spectral and seabed exposure regionalisation schemes (Fig. 8b) indicate similarity values in excess of 0.65% over 62% of the shelf area. The largest dissimilarity is again observed in the western Great Australian Bight and in Encounter Bay (on the mid shelf) where zero similarity values are observed. The seabed exposure regionalisation indicates these regions have a minimum exposure index (seabed exposure category 0), whereas the spectral regionalisation indicates these regions are high energy (spectral category 4). This suggests a key difference between the regionalisation schemes. The events which impact on the mid-outer shelf along the southern margin are likely to be large seasonal (low frequency) storms, as indicated by spectral category 4. However, the seabed exposure regionalisation (category 0) suggests these large events have little to no influence on the Australian continental shelf, probably because they occur too rarely. Regions with similarity values of 0.1 are observed on the north-west shelf and in the Gulf of Carpentaria. The dissimilarity observed in these regions is due to the Spectral scheme defining mid-energy zones (category 3), whereas the seabed exposure regionalisation scheme defines these as high-energy zones (categories 4–5). The corresponding contingency table (Table 6) indicates that high and maximum exposure seabed exposure categories (categories 4 and 5) predominantly correspond with spectral scheme categories 3 and 4. Therefore, the seabed exposure regionalisation scheme slightly overestimates the energy predicted by the spectral scheme. As a result, the agreement between the spectral regionalisation and the seabed exposure regionalisation is the poorest of the three map comparisons.

Comparison of the PDF and seabed exposure regionalisation schemes (Fig. 8c) indicate similarity values in excess of 0.65% over 79% of the shelf area. Once again, the largest dissimilarity between maps occurs in the western Great Australian Bight and Encounter Bay with similarity values of 0.1. As for the spectral to seabed exposure comparison, this is due to the seabed exposure scheme predicting these areas to have low exposure (category 0), but the PDF scheme indicates high β values (categories 3 and 5; indicating high mean and maximum bed shear stresses). Again, similar to the previous comparison, dissimilarity observed on the mid north-west shelf and in the Gulf of Carpentaria is due to the seabed exposure index overestimating exposure in comparison to the other scheme (in this case the PDF scheme). The contingency table for this comparison (Table 7) shows much better agreement between the maps at the higher energy levels than the spectral/seabed exposure comparison, and consequently, the PDF/seabed exposure map comparison shows the greatest similarity of the three map pairs.

4. Discussion

The primary aim of this study was to quantify the magnitude and frequency of exposure in response to the combined influence of waves and currents on the Australian continental shelf, and provide a regionalisation that might be used as part of a hierarchical habitat classification scheme. Three methods of characterising the magnitude and frequency of combined flow bed shear stress as a measure of exposure have been presented, and applied to regionalise the Australian continental shelf for inclusion in habitat classification schemes.

Typically, results of the three regionalisation schemes presented in this study characterising exposure on the Australian continental shelf are in good agreement (Fig. 8). For example, high-energy zones defined by the spectral regionalisation correspond to areas with large β values in the PDF regionalisation, or a high-seabed exposure index. However, as outlined in Section 3.6, there are examples where two regionalisation schemes contradict one another. These examples where two regionalisation methods supply contrasting information on the bed shear stresses provide extra information about the type of stresses that occur there. For example, areas classified as high energy by the spectral regionalisation and dominated by energy contained in the low frequency band (e.g., inner shelf of Gulf of Carpentaria, Mid shelf on the southern and western margins; Fig. 6A), are classified as low exposure zones by the seabed exposure index (Fig. 6C). These areas are impacted upon by infrequent events acting to disturb the seabed energetically on rare occasions (e.g., cyclones, or large inter-annual storms which are able to impact the seabed on mid-to-outer-shelf water depths).

An ANOVA was carried out to determine whether mean values of physical sediment properties are significantly different between categories of each regionalisation. F values (being the ratio of variances, with higher values indicating greater variance between categories than within categories) were greatest for the spectral regionalisation, for all properties (mean grain size, carbonate content, and water depth), in comparison to other methods (Tables 2–4). Therefore, of the three regionalisation schemes presented, the spectral method shows the strongest relationship to available physical sediment data. Benthic habitats are likely to respond to magnitude and frequency of exposure in a similar manner to sediments (or when sediments are disturbed). It follows that the spectral regionalisation is the best choice of these three methods for characterising oceanographic exposure on benthic habitats.

Although the spectral regionalisation has been identified as having the strongest relationship to sediment properties, each scheme presented has advantages and disadvantages. For example, the main disadvantage of the spectral method is that it is the most complex, and computationally intensive of the three methods presented. The PDF scheme has advantages in that once the shape and scale parameters of the two-layer Weibull probability distribution function have been calculated, the entire dataset is easily described by just these two parameters. The probability (and hence the average return period) of a particular magnitude bed shear stress event (e.g., the critical stress required to tear an organism from their place of attachment) can then be easily determined. Similarly, the magnitude of bed shear stress experienced during an N-year storm event may be easily calculated.

When assessing areas with only small variation in the exposure experienced, these areas may fall within one category of a regionalisation. In this circumstance, the seabed exposure index regionalisation has advantages in that it is the only one of the three methods presented which represents both the magnitude and frequency of bed shear stress at a location by one value capable of resolving differences. One approach in this situation might be to assess the total integrated energy obtained from the spectral regionalisation, and place no weighting on the frequency with which the bed shear stress occurs. Such an approach loses the ability to resolve regions often disturbed (high frequency dominated) from rarely disturbed (low frequency dominated) regions. However there are inherent differences in the trends in physical sediment properties with increasing energy between low- and high-frequency dominated regions (e.g., mean grain size shows greater increase with energy in low-frequency dominate regions than high frequency dominated regions; Table 2), which demonstrates the importance of exposure frequency to describing the benthic environment.

A secondary aim of this study was to determine whether the present day physical sediment properties are in hydraulic equilibrium with the prevailing oceanographic conditions. Porter-Smith et al. (2004) concluded that large areas of Australia's continental shelf were not in hydraulic equilibrium with present conditions. However, their method has many aspects which have been improved in this study. Firstly, the statistics presented by Porter-Smith et al. are calculated from the whole grain size grid, which includes values linearly interpolated from nearby sites and descriptive grain-size data. To remove these sources of error, the statistics calculated and presented in Tables 2–4 are computed from locations where only quantitative samples have been collected. This reduces the number of available samples from which to calculate statistics, however the number of samples within each category remains sufficient to obtain significant statistics. Secondly, the location of zero-mobility regions derived by Porter-Smith et al. (2004) is strongly dependent on the input grain size (i.e., a large error in grain size is directly transferred to a large error in the threshold velocity required for sediment mobility. If grain sizes are over-estimated, the site has a much larger probability of being classified as a zero-mobility region). To counteract this source of error, grain size is used as a measure of bed roughness only, which is a lower order influence on the calculated combined-flow bed shear stress. Therefore, results are less biased by the grain size inputs to the model. Finally, in this study, statistics are calculated at multiple energy levels using three methods to quantify the magnitude and frequency of bed shear stress or exposure. With increasing energy levels (i.e., increasing energy in the spectral regionalisation, increasing β in the PDF regionalisation, or increasing seabed exposure index), the following relationships are observed:

- Water depth decreases;
- Mean grain size typically displays a significant increase. An exception to this generalisation are those regions where high-frequency bed shear stresses dominate (defined by the spectral regionalisation), where no relationship between mean grain size and energy is observed. One could interpret this as regions dominated by synoptic or seasonal scale events (e.g., storm dominated continental shelves) have a strong positive

relationship between grain size and energy, whereas regions dominated by semi-diurnal or diurnal scale events (e.g., tidally dominated shelves) show no relationship between grain size and energy;
- Carbonate content typically displays an insignificant increase. Regions dominated by low-frequency bed shear stress events (defined by the spectral method) show no such trend.

Each of the general trends described (decreasing water depth, increasing grain size, and increasing carbonate content with increasing energy) is consistent with the concept of a graded shelf (Swift and Thorne, 1991) and Aigner's (1985) ''proximality'' diagram, in which mud content and the rate of bioturbation increase in an offshore direction (with lower energy and increasing water depth).

In addition to the application of classifying benthic habitats, another application of the quantification of exposure on Australian continental shelf is fisheries management. Animals adapted to highly dynamic seabed environments due to natural causes may not be affected by seabed disturbance by fishing (trawl and dredge) practices. Conversely, animals adapted to a stable quiescent seabed environment, if disturbed by fishing gear, may take a long time to recover. DeAlteris et al. (1999) consequently argued that the relative significance of seabed disturbance by mobile fishing gear on habitat structure and the biological community must be scaled against the magnitude and frequency of seabed disturbance due to natural causes. Thus, the analysis of exposure to oceanographic processes on Australia's continental shelf carried out in this study allows identification of problematic areas with respect to the degradation of essential habitats by mobile fishing gear. Using this argument and comparing two areas of high trawl activity in Australian waters (Torres Strait and the Gulf of Carpentaria), trawling impacts will be felt more acutely in the low energy disturbance region of the Gulf of Carpentaria, in comparison to the high energy disturbance region of Torres Strait. Comparison of how benthic communities recover in these two regions in response to trawling activity is currently underway (Butler, 2005).

Model assumptions made in the computation of the bed shear stress are likely to impact on the final regionalisation maps presented. Due to the input models used, wind generated current events and wave events are not in phase. Consequently the combined flow bed shear stress will be slightly underestimated during storm events, reducing the low-frequency energy of the bed shear stress spectrum. For example, if a storm occurs, generating bed-orbital velocities in response to waves of 0.35 m/s orbital velocity and 8 s period, and generates wind-driven currents of magnitude 0.3 m/s which is typical of mixed energy regions such as Torres Strait (Hemer et al., 2004), the combined flow bed shear stress should be 4.56 Nm^{-2}. However, if the current component is not accounted for, the bed shear stresses would be 3.89 Nm^{-2}, underestimating the combined flow bed shear stress by 15%. The presence of tidal currents will result in more complex interactions, generally reducing the resultant error.

Biota, especially benthic, can exert significant controls on bed shear stress by altering the drag, and consequently the turbulence and combined flow bed shear stress on the seabed. Biota can also stabilise or destabilise bottom sediment, thus altering the critical shear stresses of the sediments. In the present model, the seabed is treated as a uniform sandy bed over the entire continental shelf. The model parameterises bedforms being generated, increasing drag and the total bed shear stress value (Li and Amos, 2001) but rock presence, biota presence or any other differences in seabed properties is not accounted for. An example of the role biota can play on bed shear stress and disturbance is in sea grass beds; if the density of plant stems falls below a critical level, roughness will be a property of the entire stem and the sediment beneath. Consequently, turbulent flow patterns are created that will tend to erode sediments between the stems and the stems themselves. However, if the number of plant stems exceeds that critical level, currents will tend to flow over, rather than through, the sea grasses. Roughness becomes a property of the canopy of the plants, reducing turbulence (and the total combined flow bed shear stress) and fine particles will drop out of suspension and be deposited at the site (Eckman, 1983).

The results of this study indicate that the frequency of combined-flow bed shear stress events is an important parameter to be retained for habitat classification schemes. It provides some quantitative assessment of the recovery time of a population or community on the continental shelf. At present, only the spectral regionalisation retains this information as high or low frequency dominated regions, and it is this regionalisation scheme of the three methods presented which displays the strongest relationship to the sedimentology on Australia's continental shelf. An assessment of the frequency of disturbance events might be obtained using the seabed exposure index scheme if the effective frequency (the probability of occurrence of the most effective bed shear stress) were retained.

5. Conclusions

This research has identified the importance of quantifying both the magnitude and frequency of combined-flow bed shear stress in characterising the seabed exposure to oceanographic processes on the Australian continental shelf. It follows that the same variables are of importance to the characterisation of benthic habitats. When undertaking ecosystem based management of our benthic environment, such quantification of the oceanographic processes on the continental shelf is an important component which to date has been only minimally considered. A key aspect of this study is the presentation of three methods that summarise a time-series of combined flow bed shear stress into a single parameter characterising the magnitude and frequency of exposure. When time-series are available from many locations, as in this case from numerical model data, a regionalisation may be created allowing spatial comparisons of exposure to oceanographic processes to be made quantitatively. The study region in this instance was the entire Australian continental shelf, which introduces complications with regards to validation of the approach to biological data. To ultimately determine the best approach to characterising the benthic environment on the basis of oceanographic data, a higher resolution case-study testing these methods against purposely collected field habitat-type data should be carried out, preferably in regions with strong exposure gradients (e.g., cross shelf gradients, or behind sheltering obstacles such as islands or peninsulas). Only when such studies have been carried out can a 'standard' approach be adapted for marine planning and policy purposes.

Acknowledgements

The author would like to thank D. Greenslade of the Bureau of Meteorology, Melbourne for the output from the Australian wave model, O. Andersen of KMS, Denmark for output from the Australian tide model, the OCCAM team, NOC, Southampton for output from the OCCAM model, and A. Hancock of Geoscience Australia, Canberra for assistance in obtaining data from the MARS database. The manuscript was improved thanks to critical reviews by Drs. Peter Harris and Andrew Heap and two anonymous reviewers. MH publishes with the permission of the Chief Executive Officer, Geoscience Australia.

References

Aigner, T., 1985. Storm depositional systems. Lecture notes in Earth Sciences, Vol. 3. Springer, Berlin, 174pp.

Aller, J.Y., 1989. Quantifying sediment disturbance by bottom currents and its effect on benthic communities in a deep-sea western boundary zone. Deep-Sea Research I 36, 901–934.

Aller, J.Y., Todorov, J.R., 1997. Seasonal and spatial patterns of deeply buried calanoi copepods on the Amazon shelf: Evidence for periodic erosional/depositional cycles. Estuarine, Coastal and Shelf Science 44 (1), 57–66.

Bagnold, R.A., 1963. Mechanics of marine sedimentation. In: Hill, M.N. (Ed.), The Sea, Vol. 3. Wiley-Interscience, New York, pp. 507–527.

Bandemer, H., Gottwald, S., 1995. Fuzzy Sets, Fuzzy Logic, Fuzzy Methods with Applications. Wiley, Chichester, New York, 250pp.

Booij, N., Ris, C., Holthuijsen, L.H., 1999. A third-generation wave model for coastal regions 1. Model description and validation. Journal of Geophysical Research 104, 7649–7666.

Butler, A., 2005. Personal Communication. CSIRO Marine and Atmospheric Research, Cleveland, QLD, Australia.

Carruthers, T.J.B., Dennison, W.C., Longstaff, B.J., Waycott, M., Abal, E.G., McKenzie, L.J., Lee Long, W.J., 2002. Seagrass habitats of north-east Australia: models of key processes and controls. Bulletin of Marine Science 71, 1153–1169.

Cheroske, A.G., Williams, S.L., Carpenter, R.C., 2000. Effects of physical and biological disturbances on algal turfs in Kaneohe Bay, Hawaii. Journal of Experimental Marine Biology and Ecology 248 (1), 1–34.

Connell, J.H., 1978. Diversity in Tropical Forests and Coral Reefs. Science 199, 1302–1310.

Coops, H., Boeters, R., Smit, H., 1991. Direct and indirect effects of wave attack on helophytes. Aquatic Botany 41, 333–352.

Davies, P.J., 1979. Marine geology of the continental shelf of southeast Australia. Bureau of Mineral Resources Bulletin (Canberra). 195, 51pp.

DeAlteris, J., Skrobe, L., Lipsky, C., 1999. The significance of seabed disturbance by mobile fishing gear relative to natural processes: A case study in Narraganset Bay, RI. In: Benaka, L. (Ed.), Fish Habitat: Essential Fish Habitat and Rehabilitation. American Fisheries Society Symposium, pp. 224–237.

Duggins, D., Eckman, J.E., Siddon, C.E., Klinger, T., 2001. Interactive roles of mesograzers and current flow in survival of kelps. Marine Ecology Progress Series 223, 143–155.

Easton, A.K., 1970. The tides of the continent of Australia. Ph.D. Thesis. Flinders University of South Australia. Research paper no. 37. 325pp.

Eckman, J.E., 1983. Hydrodynamic processes affecting benthic recruitment. Limnology and Oceanography 28, 241–257.

Edgar, G.J., 1997. Australian Marine Life. The Plants and Animals of Temperate Waters. Reed Books, Victoria, Australia, 544pp.

Edgar, G.J., 2001. Australian marine habitats in Temperate waters. Reed New Holland, Sydney, 224pp.

Egbert, G.D., Bennett, A.F., Foreman, M.G.G., 1994. TOPEX/POSEIDON tides estimated using a global inverse model. Journal of Geophysical Research 99, 24821–24852.

Engelund, F., Hansen, E., 1967. A Monograph on Sediment Transport in Alluvial Streams. Teknisk Vorlag, Copenhagen, Denmark, 62pp.

Fader, G.B.J., Pickrill, R.A., Todd, B.J., Courtney, R.C., Parrott, D.R., 1999. The emerging role of marine geology in benthic ecology. Bedford Institute of Oceanography Science Review, 9pp.

Fonseca, M.S., Bell, S.S., 1998. Influence of physical setting on seagrass landscapes near Neaufort, North Carolina, USA. Marine Ecology Progress Series 171, 109–121.

Geoscience Australia, 2005. MARS—Australian National MARine Sediments database (http://www.ga.gov.au/oracle/mars), Geoscience Australia, Canberra, Australia.

Goodsell, P.J., Connell, S.D., 2005. Historical configuration of habitat influences the effects of the disturbance on mobile invertebrates. Marine Ecology Progress Series 299, 79–87.

Grant, W.D., Madsen, O.S., 1986. The continental shelf bottom boundary layer. Annual Review of Fluid Mechanics 18, 265–305.

Greene, H.G., Yoklavich, M.M., Starr, R.M., O'Connell, V.E., Wakefield, W.W., Sullivan, D.E., McCrea Jr., J.E., Cailliet, G.M., 1999. A classification scheme for deep seafloor habitats. Oceanologica Acta 22, 663–678.

Hagen, A., 2003. Fuzzy set approach to assessing similarity of categorical maps. International Journal for Geographical Information Science 17 (3), 235–249.

Hall, S.J., 1994. Physical Disturbance and Marine Benthic Communities: Life in Unconsolidated Sediments. Oceanography and Marine Biology: An Annual Review 32, 179–239.

Harris, P.T., 1991. Reversal of subtidal dune asymmetries caused by seasonally reversing wind-driven currents in Torres Strait, northeastern Australia. Continental Shelf Research 11 (7), 655–662.

Harris, P.T., Heap, A., Passlow, V., Sbaffi, L., Fellows, M., Porter-Smith, R., Buchanan, C., Daniell, J., 2003. Geomorphic features of the Continental margin of Australia: Report to the National Oceans Office on the production of a consistent, high-quality bathymetric data grid and definition and description of geomorphic units for part of Australia's marine jurisdiction. BMR Record 2003/030, Canberra, Australia, 141pp.

Hasselman, K. and the WAMDI Group, 1988. The WAM model—a third generation ocean wave prediction model. Journal of Physical Oceanography 18, 1775–1810.

Hemer, M.A., Harris, P.T., Coleman, R., Hunter, J., 2004. Sediment mobility due to currents and waves in the Torres Strait-Gulf of Papua region. Continental Shelf Research 24 (19), 2297–2316.

Hentschel, B.T., Larson, A.A., 2004. Growth rates of interface-feeding polychaetes: combined effects of flow speed and suspended food concentration. Marine Ecology Progress Series 293, 119–129.

Jones, H.A., 1973. Marine geology of the north-west Australian continental shelf. Bureau of Mineral Resources Bulletin (Canberra) 136, 102pp.

Jones, H.A., Davies, P.J., 1983. Superficial sediment of the Tasmanian continental shelf and part of Bass Strait. Bureau of Mineral Resources Bulletin (Canberra) 218, 25pp.

Komen, G., Cavaleri, L., Donelan, M., Hasselman, K., Hasselman, S., Janssen, P.A.E.M., 1994. Dynamics and Modelling of Ocean Waves. Cambridge University Press, Cambridge, 532 pp.

Kostylev, V.E., Todd, B.J., Fader, G.B.J., Courtney, R.E., Cameron, G.D.M., Pickrill, R.A., 2001. Benthic habitat mapping on the Scotian Shelf based on multibeam bathymetry, surficial geology and seafloor photographs. Marine Ecology Progress Series 219, 121–137.

Krebs, C.J., 1994. Ecology. Harper-Collins Publishers, New York, NY, 801pp.

Li, M.Z., Amos, C.L., 2001. SEDTRANS96: the upgraded and better calibrated sediment-transport model for continental shelves. Computers and Geosciences 27, 619–645.

Long, B.G., Pitcher, C.R., Bode, L. Mason, L.B., 1997. Relationships between the distribution and abundance of sessile epibenthos in inter-reefal areas of Torres Strait and seabed current stress and bedload partings. In: Proceedings: The Great Barrier Reef Science, Use and Management. GBRMPA, Townsville, p. 191.

McCave, I., 1971. Wave effectiveness at the seabed and its relationship to bedforms and deposition of mud. Journal of Sedimentary Petrology 41 (1), 89–96.

Monserud, R.A., Leemans, R., 1992. Comparing global vegetation maps with the Kappa statistic. Ecological Modelling 62, 275–293.

Porter-Smith, R., Harris, P.T., Andersen, O.B., Coleman, R., Greenslade, D., Jenkins, C.J., 2004. Classification of the Australian continental shelf based on predicted sediment threshold exceedance from tidal currents and swell waves. Marine Geology 211, 1–20.

Roff, J.C., Taylor, M.E., Laughren, J., 2003. Geophysical approaches to the classification, delineation and monitoring of marine habitats and their communities. Aquatic Conservation-Marine and Freshwater Ecosystems 13, 77–90.

Swift, D.J.P., Thorne, J.A., 1991. Sedimentation on continental margins: I. A general model of shelf sedimentation. Special Publication of the International Association of Sedimentology 14, 3–31.

Thomsen, M.S., Wernberg, T., Kendrick, G.A., 2004. The effect of thallus size, life stage, aggregation, wave exposure and substratum conditions on the forces required to break or dislodge the small kelp *Ecklonia radiata*. Botanica Marina 47 (6), 454–460.

Visser, H., de Nijs, T., 2006. The Map Comparison Kit. Environmental Modelling and Software 21 (3), 346–358.

Warwick, R.M., Uncles, R.J., 1980. Distribution of benthic macrofaunal associations in the Bristol Channel in relation to tidal stress. Marine Ecology Progress Series 3, 97–103.

Webb, D.J., Cuevas, B.A., Coward, A.C., 1998. The first main run of the OCCAM global ocean model. Internal Report of James Rennell Division, Southampton Oceanography Centre, UK, 50pp. See also: http://www.noc.soton.ac.uk/JRD/OCCAM

Wernberg, T., Thomsen, M.S., 2005. The effect of wave exposure on the morphology of *Ecklonia radiata*. Aquatic Biology 83 (1), 61–70.

Wilks, D.S., 1995. Statistical Methods in the Atmospheric Sciences. Academic Press, London, 464pp.

Wolanski, E., Ridd, P.J., Inoue, M., 1988. Currents through Torres Strait. Journal of Physical Oceanography 18, 1535–1545.

Wolman, M.G., Miller, J.P., 1960. Magnitude and Frequency of Forces in Geomorphic Processes. Journal of Geology 68, 54–74.

Yalin, M.S., 1963. An expression for bedload transportation. Journal of Hydraulics Division, Proceeedings ASCE 90, (HY5), 105–119.